Published in final edited form as:

Int J Hyperthermia. 2018 December ; 34(8): 1316–1328. doi:10.1080/02656736.2018.1430867.

Magnetic hyperthermia therapy for the treatment of glioblastoma: a review of the therapy's history, efficacy and application in humans

Keon Mahmoudi[a], **Alexandros Bouras**[a], **Dominique Bozec**[a], **Robert Ivkov**[b], and **Constantinos Hadjipanayis**[a,c]

[a]Department of Neurosurgery, Brain Tumor Nanotechnology Laboratory, Tisch Cancer Institute at Mount Sinai, New York, NY, USA

[b]Department of Radiation Oncology and Molecular Radiation Sciences, Johns Hopkins University School of Medicine Baltimore, MD, USA

[c]Department of Neurosurgery, Mount Sinai Beth Israel, New York, NY, USA

Abstract

Hyperthermia therapy (HT) is the exposure of a region of the body to elevated temperatures to achieve a therapeutic effect. HT anticancer properties and its potential as a cancer treatment have been studied for decades. Techniques used to achieve a localised hyperthermic effect include radiofrequency, ultrasound, microwave, laser and magnetic nanoparticles (MNPs). The use of MNPs for therapeutic hyperthermia generation is known as magnetic hyperthermia therapy (MHT) and was first attempted as a cancer therapy in 1957. However, despite more recent advancements, MHT has still not become part of the standard of care for cancer treatment. Certain challenges, such as accurate thermometry within the tumour mass and precise tumour heating, preclude its widespread application as a treatment modality for cancer. MHT is especially attractive for the treatment of glioblastoma (GBM), the most common and aggressive primary brain cancer in adults, which has no cure. In this review, the application of MHT as a therapeutic modality for GBM will be discussed. Its therapeutic efficacy, technical details, and major experimental and clinical findings will be reviewed and analysed. Finally, current limitations, areas of improvement, and future directions will be discussed in depth.

Keywords

Magnetic hyperthermia therapy; magnetic nanoparticles; glioblastoma; convection enhanced delivery; alternating magnetic field

CONTACT: Constantinos Hadjipanayis, constantinos.hadjipanayis@mountsinai.org, Department of Neurosurgery, Brain Tumor Nanotechnology Laboratory, Tisch Cancer Institute at Mount Sinai, New York, NY, USA.

Disclosure statement

The authors declare the absence of any commercial or financial relationships that could be construed as a potential conflict of interest.

Introduction

Glioblastoma (GBM) is a devastating form of brain cancer that is universally lethal. GBM is the most common primary brain cancer in adults and the most aggressive according to the World Health Organization's classification (WHO grade IV high-grade glioma) of brain tumours [1]. It accounts for 12–15% of all brain tumours and has an incidence of 2–3 in 100,000 [2–4]. The standard of care for patients with GBM begins with maximal surgical resection, when possible, and continues with a combination of radiation therapy (RT) and chemotherapy followed by chemotherapy alone [5]. The tumour almost always recurs locally due to infiltrating cancer cells which reside away from the tumour bulk [6,7]. These cells are located beyond the contrast enhancing tumour visualised on magnetic resonance imaging (MRI) and are difficult to resect since they reside among healthy cells. The infiltrating cancer cells are known to be resistant to both chemotherapy and RT [8–10]. Recurrent tumours are especially resistant to therapies and difficult to treat [11]. The median survival after surgical resection, followed by RT and chemotherapy (temozolomide (TMZ)), is 14.6 months, and the median progression-free survival is 6.9 months [5]. The 2-year and 5-year survival rates are 26.5% and 9.8%, respectively [5,12]. The median survival after first tumour recurrence is approximately 6 months [13].

Due to the infiltrative nature of GBM and lack of durable and effective therapies, new treatment approaches are urgently needed. Recently, in an effort to achieve a maximal safe resection of the contrast-enhancing tumour, fluorescence-guided surgery (FGS) using 5-aminolevulinic acid (5-ALA) has been introduced in the surgical treatment of patients with GBM [14]. 5-ALA is the first-ever fluorescing agent which has been approved by the US Food and Drug Administration (FDA) for enhanced visualisation of malignant tissue during GBM surgery [15].

Hyperthermia therapy

Hyperthermia therapy (HT) is defined as a treatment approach where the temperature in a local region of the body is elevated above baseline to achieve a therapeutic effect [16]. HT has been studied for over a century as a treatment for cancer [17]. The goal of HT is for more than 90% of the target region to receive the minimum effective hyperthermia dose [18,19]. The total energy delivered is measured using a widely accepted metric in which the duration of exposure is normalised to the base effective temperature of 43 °C (CEM43) [19]. An important distinction between HT and generalised fever is that HT elevates the core body temperature without changing the physiological set point [20]. However, during localised HT, the core body temperature does not increase to the same extent as the temperature in the treatment area [21].

An increase in the local temperature to values between 40 and 44 °C is sufficient to negatively impact cancer growth [22,23]. The interactions of heat with RT and chemotherapy and the effects of heat on cancer cells have already been described [24,25]. It has been reported that moderate HT (45 °C) induced apoptosis in a human GBM cell line and in a murine animal glioma model [26]. It has additionally been demonstrated *in vitro* that a temperature-dependent induction of apoptosis occurred when multiple glioma cell lines were subjected to a range of hyperthermia conditions (43–47 °C) [27].

Heat shock proteins (HSPs) play a vital role in the resistance of cancer cells to HT [20]. Healthy and cancer cell HSPs participate in the cellular response to injury from DNA damage and RT [28–30]. HSP27, 70, 72 and 90 have been identified as key proteins that are constitutively overexpressed in glioma cells and other cancers [24,31,32]. Novel immunotherapeutic agents may potentially exploit this overexpression of HSPs by activating the immune system to specifically target cancer cells [33].

HT has been described as a potential chemosensitiser. There are several proposed mechanisms of HT-induced chemosensitisation, including generation of a transient disruption of the blood–brain barrier (BBB), increased blood flow that accompanies hyperthermia conditions, interference with DNA repair mechanisms, heat-induced damage to ATP-binding cassette (ABC) transporters, changes in tumour cell drug metabolism, and an impaired ability to withstand apoptotic pathways [23,25,34–38].

HT also plays an important role in radiosensitisation by affecting the religation step of base excision repair following RT-induced DNA damage, suppressing the protein kinase B (AKT) signalling pathway, and interfering with the interaction between damaged DNA and DNA-repair machinery [25,38–41]. Cells that are typically resistant to RT, such as hypoxic or plateau-phase cells, are more susceptible to HT [42].

HT can be applied via whole body, regional and localised methods. Localised HT appears to be the most effective for GBM due to the treatment's focus on the tumour region [43]. Localised HT also has less side effects compared to the other modalities [44]. Methods of localised HT for GBM therapy include microwaves, ultrasound, radiofrequency, laser and magnetic nanoparticles (MNPs) [24].

Magnetic hyperthermia therapy

Magnetic hyperthermia therapy (MHT) was first attempted in 1957 to treat cancers that had metastasised to the lymph nodes, and it built upon the principles of localised HT by using MNPs and incorporating an alternating magnetic field (AMF) to generate heat [45]. In MHT, heat is produced after local deposition of MNPs and subsequent application of an external AMF (Figure 1 [46]). In general, all magnetic materials can generate heat via hysteresis losses when they are exposed to AMFs. The heating capacity depends upon the properties of the magnetic material and the AMF parameters. MNPs can also generate heat when they are exposed to AMFs. However, for magnetic nanostructured materials, the heating efficacy is based on a more complex relationship between the intrinsic time-dependent relaxation processes of the nanoparticle (NP) magnetic moments and the time-scale of the oscillating AMF field vector [47–50]. While there has been considerable debate regarding the mechanisms responsible for heat generation by MNPs, consensus is emerging that the most important contribution is provided by magnetic hysteresis losses.

MHT has been attempted *in vivo* to treat a variety of cancers including lung, breast, prostate, spine, brain, head and neck, pancreas, and liver [18,51–57]. In Europe, MHT was approved as an adjuvant therapy for recurrent GBM in combination with RT in 2012 [58].

Magnetic nanoparticle heating efficacy and thermal modelling

MHT effectiveness depends upon delivery of an appropriate thermal dose [18]. The lowest thermal dose that is delivered to any tumour region dictates the overall response to the treatment [19,59]. At low heating power, localised MNP distribution produces a more pronounced anti-tumour effect compared to a more uniform MNP distribution [60]. The opposite relationship between MNP distribution and anti-tumour effect occurs at high heating power [60].

For any MNP construct, thermal modelling is critical for understanding the heating efficacy at the cellular level. Pennes' bioheat transfer equation (BHTE) can be used to predict temperature profiles during local hyperthermia [61,62]. Despite the development of more accurate temperature prediction models, BHTE can still be applied to almost every case of thermal modelling [63]. When applying BHTE, the specified magnetic field strength, frequency, background temperature, estimated average perfusion, MNP concentration, and distribution in the target tissue yield an energy term which is then used to estimate the power absorption and temperature distribution within the target region.

Prior to the application of MHT in phantoms or patients, safety and effectiveness must be ensured by generation of an accurate and reliable treatment plan. Specialised software can overlay an MRI acquired before MNP administration to a post-MNP injection computed tomography (CT) image to determine the distribution of MNPs in patients with GBM [64]. The software can then calculate the expected heat distribution within the brain at various magnetic field amplitudes [64]. One group has validated a coupled electromagnetic and thermal model to predict dynamic and thermal distributions during AMF treatment [65]. Variables such as tissue density, specific heat of tissue, thermal conductivity of tissue, and metabolic heat generation rate were used in a variation of the BHTE equation. Phantoms and a heterotopic (flank) murine adenocarcinoma animal model have both validated the simulation. However, this model would have to be revalidated in GBM animal models before application to GBM patients.

Accurate treatment planning can allow for generation of a temperature–distance diagram which can provide better visualisation of the thermal gradient present in the tumour region compared to single-point thermometry. Thermal modelling that is in agreement with physical temperature measurements can complement focal thermal monitoring [66]. The limitation in producing a reliable thermal model is that thermal dosimetry also depends on variations in tissue physiology [66]. Alternatively, MR thermometry can provide real-time temperature monitoring without requiring accurate heat transfer models or knowledge of local particle concentrations [66].

Administration of magnetic nanoparticles for magnetic hyperthermia therapy

Common delivery methods of MNPs for MHT application in humans include systemic administration and direct intratumoural injection. Systemic MNP administration is typically avoided for MHT of GBM due to the presence of the BBB. In the healthy brain, the BBB preserves normal brain function by maintaining a homeostatic neuronal environment [67]. This highly selective barrier prevents exposure of brain tissue to many possibly harmful

compounds. The selectivity of the BBB can be altered by pathological conditions such as stroke, epilepsy and brain tumours [68,69]. High-grade tumours, such as GBM, have an elevated metabolic demand which creates hypoxic regions within the tumour and leads to abnormal angiogenesis. These abnormal vessels comprise the blood–brain tumour barrier (BBTB). Although the BBTB is more permeable than a healthy BBB, it is still very selective, rendering it impermeable to many chemotherapeutic agents [69]. The permeability of the BBB and BBTB can be increased with exposure to RT [70]. Treatment of GBM with RT and adjuvant chemotherapy exploits this phenomenon. After a period of time following RT, both the BBB and BBTB return to pre-treatment permeability levels [71].

Direct intratumoural administration of MNPs is preferred for MHT of GBM due to the high localised accumulation of MNPs that is required for sufficient heat generation in tumours and efficacy. In a phase II study of MHT in patients with recurrent GBM, MNPs were stereotactically injected directly into tumours [58]. Concerns of MNP leak back have questioned this method of direct delivery for GBM.

Convection-enhanced delivery (CED) is a local delivery method that has many advantages for GBM therapy applications, including MHT. CED, which was first proposed by Bobo *et al.*, allows a therapeutic to be directly delivered to a specific intracranial region [72]. CED is typically achieved by implantation of one or more catheters in the brain parenchyma to perform a pressure-dependent infusion at a constant predetermined flow rate controlled by an external pump [73–75]. Most regions of the brain are accessible via CED [76–78]. CED bypasses the BBB and results in robust local accumulation of a therapeutic in the brain parenchyma while avoiding systemic exposure and minimising toxic effects. However, the heterogeneous nature of GBM complicates the uniform delivery of therapeutics, as some tumour regions may metabolise a therapeutic at a faster rate compared to other tumour areas [79]. In some instances, leak back (reflux) of the therapeutic may occur. Reflux is counterintuitive to the principles of CED, and if an increase in infusion volume is subsequently attempted, an increase in distribution volume will not be observed [74].

MNPs are ideal candidates for CED application. Their small size allows for optimal distribution within the target brain region. With real time MR imaging, MNP delivery into the brain by CED can be closely monitored and adjusted in case of non-optimal catheter placement or reflux along the catheter tract [73,76,80]. MHT is often performed with iron-oxide MNPs (IONPs) due to their high heating capacity [81]. Examples of IONPs include magnetite and its oxidised counterpart, maghemite [82,83]. IONPs delivered directly to the rodent brain via CED can be visualised via MRI several months after treatment [84]. Intracranial MNP CED has been successfully performed in multiple rodent GBM models and in healthy canines [84–87].

Magnetic nanoparticle toxicity

The toxicity of MNPs is dependent on a variety of factors including concentration, chemical composition and physical properties such as size, shape and surface coating [88]. Idiosyncratic reactions can also lead to MNP toxicity. Different tissues metabolise MNPs at varying rates resulting in variable toxicity [89]. A lower metabolic rate within a particular tissue may lead to sedimentation of MNPs and a higher effective concentration, potentially

leading to enhanced toxicity [90]. MNPs composed of gold, cobalt, nickel, cadmium, zinc and silver can be more toxic than iron-oxide and titanium [88]. The size and shape of MNPs is also important as larger molecules may aggregate, coagulate and evoke a toxic response [88]. Surface coatings such as dextran can prevent coagulation and reduce MNP toxicity.

MNPs have been utilised as MRI contrast agents in many studies and their safety has been demonstrated. In one study, labelling of haematopoietic and mesenchymal stem cells *in vitro* with 100 μg/ml ferumoxide (SPION MRI contrast agent) did not alter cell viability or differentiation capacity [91]. In another study, human embryonic stem-cell-derived cardiomyocytes labelled with ferumoxide at a concentration of 50 μg/ml were not shown to have any reduction in cell viability compared to stem cells not labelled with IONPs [92]. Furthermore, in a U87 rat glioma study, no evidence of animal toxicity was found after systemic administration of 5 or 25 μg of ferumoxtran-10 (dextran-coated ultra-small SPION MRI contrast agent) [93]. Intracranial CED of MNPs has been safely applied to rodent GBM models with no reported short- or long-term side effects [84,86,87].

Few human studies have reported significant adverse effects of MNPs [88,94]. In a review of 37 phase I to III ferumoxtran-10 clinical studies (1777 total participants), the most common mild side effects after intravenous MNP administration were back pain, pruritus, headache and urticaria [95]. In seven cases, however, severe side effects were observed such as anaphylactic shock, chest pain, dyspnoea, skin rash, decreased oxygen saturation and hypotension. Application of MNPs for MHT in GBM patients was associated with side effects such as sweating, tachycardia, short-term blood pressure fluctuations, mild headaches, seizures and worsening of already-existing hemiparesis [58,64]. Due to the limited amount of data on MNP toxicity in humans, more studies are necessary to determine the side effect profile of MNPs when they are delivered to the human brain.

Magnetic hyperthermia therapy effectiveness

A limited number of studies have explored the application and efficacy of MHT with *in vitro* and *in vivo* glioma models. The characteristics of these studies are summarised in Tables 1 and 2.

***In vitro* studies—**The antitumour effect of MHT on gliomas has been studied for the past twenty years. One group reported the use of magnetite cationic liposomes (MCLs) to generate intracellular HT in T-9 rat glioma cells *in vitro* [96]. An optic fibre thermometer was placed at the centre of the gel. Complete tumour cell death was observed after 40-min of MHT application at 43 °C. In their second *in vitro* study, they found that MHT induced HSP-70 expression in the cancer cells [97]. After 30-min of MHT at 42 °C, the T-9 glioma cells displayed cell apoptosis and necrosis. The necrotic cells were purified to extract HSP-70 which was subsequently implanted into rats to confer immunity against a T-9 glioma challenge. More recently, another group used polyethylene glycol-based magnetic hydrogel nanocomposites to produce a pronounced heating effect (60.7–79.6 °C) on M059K GBM cells, resulting in thermoablation of the cells [98]. The surface temperature of the gel was monitored using an infra-red camera. A third group demonstrated the apoptotic and necrotic effects of MHT *in vitro* on U251 glioma cells [99]. Iron oxide MNPs were utilised

for MHT application and a digital thermometer was used every 5-min for temperature recording. A statistically significant inhibition of glioma cell proliferation with a concentration-dependent relationship to the IONP concentration was reported.

Animal studies—The earliest results of MHT application in an animal glioma model were published in 1997 [21,100]. In this preliminary *in vivo* study, MCLs were incubated with T-9 rat glioma tumour cells for 8 h before subcutaneous implantation into the femoral region of rats [100]. After three 60-min MHT sessions applied at intervals of 12 hours, all the glioma cells were killed. A subcutaneous fibre optic thermometer was used for intratumoural temperature measurements. In a later study, the same group subcutaneously implanted T-9 rat glioma cells into the femoral region of rats followed 11 days later by intratumoural injection of MCLs using an infusion pump [101]. The first MHT session was performed 24-h after the MNP infusion for 30 min. MHT was repeated up to two more times at additional 24-h intervals. Complete tumour regression was found in the majority of tumour bearing rats from the groups receiving two or three MHT sessions.

The same group published a third study demonstrating the induction of CD8 and CD4 T cells following MHT treatment in two groups of rats [102]. After T-9 rat glioma cells were subcutaneously implanted in the femoral region, the first group received no MHT (control group) while the second group received 30-min of MHT every day for three days (treatment group). Close to 90% of the rats in the treatment group had complete tumour regression while the remaining animals had a significant reduction in tumour size. The rats that had complete tumour regression underwent a second subcutaneous implantation of T-9 cells three months later in the right femoral region. These mice demonstrated reduced tumour growth compared to the control group. In their fourth study, this group demonstrated that T-9 rat glioma cells subcutaneously implanted into the femoral region released tumour-specific HSP-70 following MHT [97]. After 3 weeks of weekly 30-min MHT sessions at 42 °C, the rats that were immunised with T-9-derived HSP-70 had significantly reduced tumour growth compared to the rats that received no immunisation. The same research group also used an athymic nude mouse heterotopic glioma model to test a tumour specific antibody-conjugated magnetoliposome which can target glioma cells both *in vitro* and *in vivo* [103]. In this study, U251-SP cells were subcutaneously implanted into the femoral region of mice followed by injection of MCLs. Both the control group and treatment group received MCLs, but only the treatment group underwent MHT. MHT was performed daily for 30-min intervals over three days. Two weeks after MHT, there was no tumour growth in the treatment group, whereas the control group exhibited tumour progression.

The same group then utilised stick type carboxymethylcellulose (CMC) magnetite to test MHT efficacy in an orthotopic rat glioma model [104]. The temperature of the tissue beneath the scalp was measured with a fibre optic probe. The CMC-magnetite stick had a higher concentration of magnetite compared to the MCLs and had an improved targeting ability. T-9 rat glioma cells were intracranially implanted in rats. Eight days later, a 0.5 cm CMC-magnetite stick was implanted into the tumour. The first 30-min MHT session was administered 24-h after CMC-magnetite stick implantation. Animals underwent up to three MHT sessions, with rats that received three sessions having a significantly prolonged survival compared to animals that received no treatment or one MHT session.

A second group has also utilised an orthotopic rat glioma model (RG-2 rat glioma cells) [54]. MNPs were deposited intratumourally via CED on day 4 post-tumour implantation followed by two 30-min MHT sessions on days 4 and 6. A single fibre optic temperature probe was inserted into the tumour via a catheter. Intratumoural temperatures of 39–47 °C were achieved during the MHT sessions. Carboxydextran-coated and aminosilane-coated IONPs were both used for MHT. The treatment group that received the aminosilane-coated IONPs and MHT demonstrated a significant decrease in tumour cell proliferation, large regions of tumour necrosis, and increased overall animal survival. This is an indication that the MNP coating plays an important role in MHT efficacy. A reactive astrogliosis, but no neuronal degeneration, was observed in brain tissue adjacent to the MHT treated tumours.

The efficiency of MHT after direct infusion of maghemite NPs was demonstrated in an extracranial rat glioma model [105]. C6 glioma cells were extracranially implanted into rats and allowed to grow for 14 days before inoculation of the maghemite MNPs. MHT was then performed for 20 min. Temperature measurements were not performed in this study. After treatment, histological analysis of the animal's brain revealed extensive tumour tissue damage and dissolution.

In a more recent *in vivo* MHT study, U251 human glioma cells were implanted into the right lower limb of rats [99]. Rats in the control group did not receive MNPs or MHT. Rats in the first treatment group received MNPs at a concentration of 4 mg/ml without MHT. Rats in the second treatment group received MNPs at concentrations of 2–8 mg/ml with MHT. Temperature measurements were not reported in this study. All animals were sacrificed two weeks after MNP implantation and their tumours were analysed histologically. The tumours from the second treatment group receiving the highest concentration of MNPs (8 mg/ml) had more significant haemorrhage and tumour necrosis.

Magnetic hyperthermia therapy in combination with adjuvant therapies—The addition of adjuvant treatments to MHT, such as RT and chemotherapy, can have a synergistic effect against GBM. The general principles of radio- and chemosensitisation described earlier for HT also apply to MHT.

Combination of MHT with chemotherapy and/or RT has already been studied to a limited extent [106,107]. Phase I and II studies of MHT in combination with RT have been performed in patients with recurrent GBM (see below).

Fe(Salen) NPs are a type of MNP that have intrinsic chemotherapeutic and heating properties [108]. Their chemotherapeutic effect can be exhibited regardless of AMF exposure. In a chemotherapy and MHT combination study, Fe(Salen) NPs were used to generate heat under AMF influence [106]. U251 human glioma cells were implanted into the legs of female nude mice followed by stereotactic implantation of Fe(Salen) NPs, carmustine (BCNU) or saline at a volume of 10 μl. Temperature measurements were obtained using a subcutaneous fibre optic thermometer. An AMF was applied for 20-min and temperatures above 43 °C were observed in the Fe(Salen) NP group, whereas the measured temperatures in the other two groups did not exceed 38 °C. The mice in the Fe(Salen) NP group demonstrated the least tumour growth among all the treatment groups

exposed to an AMF. Fe(Salen) NPs were found to generate reactive oxygen species and reduce tumour cell viability in a dose dependent fashion after exposure to an AMF.

In another study, U251 human glioma cells were initially treated *in vitro* with silver nanocrystals (AgNPs), maghemite MNPs or a combination of both, followed by RT and AMF treatment [107]. All treatment groups received 0–6 Gy of RT and were then exposed to an AMF for 15 min. A fibre optic temperature sensor was used to monitor the temperature. A temperature of 42 °C was reached in the groups receiving MNPs and AMF treatment. The tumour cells that were treated with a combination of AgNPs and MNPs followed by the highest dose of RT and subsequent AMF exposure revealed the lowest overall tumour cell survival. AgNPs were used in combination with MNPs to produce an enhanced cytotoxic effect when simultaneously exposed to an AMF after RT. The additional cytotoxic effect observed with AgNPs was attributed to the intracellular translocation of silver ions which interfered with post-IR and post-MHT cellular repair processes along with induction of G_2/M cell phase arrest.

MHT has additionally been used in combination with gene therapy in a heterotopic rodent glioma model [109]. In this study, U251-SP human glioma cells were implanted into the right flanks of female athymic mice followed by intratumoural injection of a pGadTNF plasmid containing the human tumour necrosis factor alpha (TNF-α) gene under the control of the growth arrest and DNA damage (gadd) 153 promoter. The gadd 153 gene has previously been described as a DNA damaging reagent [110]. MCLs were then injected intratumourally followed 24-h later by 30 min of AMF exposure. Intratumoural temperature was monitored using a fibre optic probe. MHT was maintained at 46 °C during the entire treatment duration. Combination of gene therapy and MHT resulted in higher levels of TNF-α expression and virtually no tumour growth compared to the other treatment groups in which gene therapy or MHT were administered alone. The increased TNF-α levels observed after the combination therapy were attributed to the MHT-induced intratumoural activation of the TNF promoter.

AMF generators for GBM applications

For MHT application, an external AMF generator is required. A common feature among the different AMF generators that have been designed for MHT is the solenoid coil [111]. When the target region is placed within the coil, it is subjected to a uniform AMF field. Many groups have designed their own solenoid coils, but commercially available coils also exist for AMF generation (e.g. Nanoscale Biomagnetics, Zaragoza, Spain; Magforce Nanotechnologies AG, Berlin, Germany) [54,100,112,113]. The same type of coil used for *in vitro* or *in vivo* experiments can be built larger to accommodate humans. Some limitations of simple solenoid coils are that a uniform magnetic field is provided for only a limited volume within the coil, and they can have asymmetric field distribution through transverse planes [114]. One group has designed an improved solenoid coil that has a higher efficiency and homogenous field uniformity within a volume of interest [114]. This coil has wide planar turns, magnetic concentrators on both ends, and wider leads for reduced power and voltage losses. As described earlier, thermal modelling is necessary to determine the appropriate field parameters for maximal treatment effect.

In Europe, a novel hyperthermia and thermoablation system (MFH 300F NanoActivator®; MagForce Nanotechnologies AG, Berlin, Germany) has been approved for clinical application of MHT including use in GBM patients [58,64,115–118]. The treatment area of the AMF applicator has a diameter of 20 cm, a magnetic field strength of up to 18 kA/m, and a field frequency of 100 kHz [115]. A prototype of the machine demonstrated energy absorption rates that are sufficient for either hyperthermia or thermoablation [115]. The generator is used in conjunction with a proprietary temperature simulation software for treatment planning (NanoPlan®; MagForce Nanotechnologies AG, Berlin, Germany). The distribution of the injected MNPs is measured by CT scan. A three-dimensional image which includes the tumour, the MNP deposits and the thermometry catheter is generated. The BHTE is used to provide an estimate of the temperature distribution in the tumour area for a given AMF amplitude. Alteration of the AMF parameters can result in simulation of different treatment plans and is used to determine the optimal AMF amplitude to achieve the desired temperature distribution within and around the tumour [119].

Quality assurance guidelines for proper superficial HT have been published by the European Society for Hyperthermic Oncology (ESHO) [120,121]. These guidelines identify clinical conditions which ensure efficacious HT for a given tumour volume [120]. ESHO guidelines also include detailed instructions on proper documentation of HT applicator performance to generate reproducible HT treatments of uniformly high quality [121].

AMF safety

Although the clinical use of AMF generators is mostly regarded as safe, the upper limits of the magnetic field that can be safely tolerated by humans are not accurately defined [122]. The Brezovich criterion refers to self-imposed limits that were initially created to minimise any potential harm from the use of AMF generators in humans [123]. More recently, a new upper limit was hypothesised that was one order of magnitude greater than the Brezovich criterion [124]. However, only healthy volunteers were used to establish both criteria. These limits depend on specific magnetic field parameters (e.g. field frequency and amplitude) and tissue properties (e.g. conductivity and volume exposed). Therefore, the proposed limits should not be substituted for the proper measurement of clinical tolerability under therapeutic conditions [125]. Currently, most MHT applicators approved for human use generate magnetic fields with a frequency range of 0.05–1.2 MHz and an amplitude range of 0–5 kA/m [125]. However, in the clinical trials where MHT was used in the treatment of GBM patients, an AMF with intensity of 18 kA/m and frequency of 100 kHz was safely applied to the brain in multiple sessions.

Magnetic hyperthermia therapy in clinical trials

A small number of clinical trials using MHT as a treatment modality have been conducted in GBM patients in recent years, and they have promising results (Table 3). In a phase I study, 14 patients diagnosed with primary or recurrent GBM received combination therapy of RT and adjuvant MHT [64]. Aminosilane-coated superparamagnetic IONPs at a concentration of 112 mg/ml were directly injected into the non-resected tumours under stereotactic guidance. The median injected volume was 3.0 ml which corresponded to a median of 0.2

ml of MNPs per ml of tumour volume. MHT was performed for 60-min twice a week for an average of six sessions. The AMF used for MHT had a frequency of 100 kHz and a variable field strength of 2.5–18 kA/m. A closed-end thermometry catheter was placed in the tumour area after injection of the MNPs. The average intratumoural temperature reached was 44.6 °C. RT was administered at single fractions of 2 Gy for a median total of 30 Gy. Treatment safety with no major side effects or neurological deficits was demonstrated. The MNPs generated localised HT, and local tumour control was achieved. In the first post-mortem study of three patients with GBM who underwent MHT, MNPs and their aggregates were mainly internalised by macrophages within the tumour mass and to a lesser degree by GBM cells [126]. The bulk of the MNPs were aggregated in the necrotic tumour mass with macrophages responsible for phagocytosis of the particles present at the aggregate borders. It was suggested that internalisation of MNPs by macrophages can be promoted by MHT application. It can be inferred from these findings that macrophages play an important role in the clearance of MNPs within GBM. No adverse effects from the injected MNPs were observed.

In a larger phase II study involving 59 patients with recurrent GBM, RT combined with MHT resulted in a significantly prolonged overall survival following diagnosis of tumour recurrence compared to a reference group [58]. The median overall survival following primary tumour diagnosis was also prolonged. IONPs were directly injected intratumourally under stereotactic guidance at a concentration of 112 mg/ml with a median volume of 4.5 ml corresponding to a median concentration of 0.28 ml of MNPs per ml of tumour volume. The AMF parameters and the treatment plan used were identical to those applied to the phase I study, and an average intratumoural temperature of 51.2 °C was achieved during MHT. No long-term side effects were observed except for temporary worsening of already-existing hemiparesis in approximately 20% of patients. Key parameters of iron metabolism were analysed before and after delivery of the MNPs in a subset of patients. No evidence was found that the infused iron was released from the tumour mass or metabolised in the liver. In Europe, these findings led to the approval of a MNP compound (NanoTherm® AS1; MagForce Nanotechnologies AG, Berlin, Germany) for MHT application in combination with RT in patients with recurrent GBM [119].

One patient who underwent surgical resection of a recurrent GBM tumour developed new clinical symptoms 14 weeks after receiving six 1-h MHT sessions with NanoTherm® and concomitant RT [127]. A CT scan of the brain revealed a ring-enhancing lesion in the resection cavity with extensive surrounding oedema indicative of an abscess. A subsequent surgery was performed to remove the lesion, and histopathology revealed sustained necrosis and a large amount of the injected MNPs without any signs of tumour recurrence. Negative results from microbiological testing and the detection of a variety of immune cells led the authors to conclude that MHT in combination with RT can result in a strong inflammatory response within the resection cavity with imaging characteristics similar to an abscess [127].

Current drawbacks to magnetic hyperthermia therapy in humans

A few drawbacks have been reported regarding MHT use for patients with GBM. One drawback is the removal of dental fillings, implants and crowns, as well as other metallic

materials within 40 cm of the treatment area prior to AMF exposure [58]. Implantation of pacemakers and defibrillators is a contraindication due to the electromagnetic interference caused by an AMF [128]. Another drawback is the inability to monitor the tumour response to treatment by MRI due to artefacts generated by the high concentration of the injected MNPs. Instead of MRI, fluoroethyl-tyrosine positron emission tomography/computerised tomography (FET-PET/CT) and single-photon emission computerised tomography (SPECT) can be used to monitor tumour growth and recurrence in these patients [58,127]. However, MRI can still detect new tumour lesions either outside the MNP deposit areas or in the contralateral brain hemisphere. Furthermore, as discussed before, stereotactic injection may not be the best delivery option for the MNPs due to anecdotal reports of leak back of the MNPs along the stereotactic site and inadequate distribution within and around the tumour area. Despite these drawbacks, the benefits seen in the limited number of clinical trials using MHT as a treatment modality for GBM patients indicate that MHT may have a larger impact in the future care of GBM patients.

Some obstacles remain for optimal MHT application in GBM, such as accurate intratumoural heating and precise temperature control at the tumour site [129]. Accurate local heating within the tumour mass should be ensured, as extreme temperature elevations may lead to damage of surrounding healthy brain tissue and insufficient tumour heating may lead to inadequate treatment and subsequent tumour recurrence. Single point thermometry makes it difficult to quantify the average temperature increase of an entire tumour mass, especially with larger tumours, as their temperature change may not be homogenous. Multiple point thermometry is hindered by the high spatial resolution (<0.5 cm) that is necessary for accurate temperature modelling [130]. Blood vessels in the tumour region further complicate accurate temperature modelling as they lead to irregular cooling caused by blood flow in the treatment field and temperature nonuniformity [130]. Another obstacle is the presence of the thermal conductivity-associated temperature gradient at the AMF boundary.

These obstacles can be potentially overcome with shorter duration, higher-temperature MHT sessions [131]. Even with proper delivery of MNPs, the fluid nature of the infusate along with the small size of each individual MNP leads to the potential for redistribution of the MNPs after MHT [132]. Accurate targeting and localisation of the MNPs to the tumour site should be improved, as it is essential in mini-mising any possible adverse effects that may arise from the heating of eloquent areas within the brain. A temperature feedback control system that adjusts the AMF parameters in real-time may overcome some of these obstacles, however, single-point thermometry would lead to inaccurate thermal dose calculations [18]. The biophysical and biochemical properties of MNPs used for MHT, such as size and coating, as well as the AMF parameters, such as frequency and field amplitude, should also be considered and adjusted for optimised GBM therapy [129].

Future direction of magnetic hyperthermia therapy

Despite the demonstrated efficacy of MHT *in vitro*, in animal models, and in humans, many obstacles remain that have hindered this therapeutic modality from becoming part of the standard of care for patients with GBM. The key to overcoming these obstacles is the

development and utilisation of MNP constructs that generate sufficient heat at lower magnetic field amplitudes which are clinically relevant. A lower concentration of iron may permit the use of MRI for follow-up in GBM patients vs. CT due to decreased field inhomogeneities. A MNP construct that demonstrates high heating efficacy at lower field strengths may obviate the need for removal of dental fillings, crowns and implants prior to MHT. Delivery of MNPs to the tumour site is an additional challenge. CED appears to be the most efficient delivery method for application to GBM due to its localised concentration and reduced backflow of the MNPs. CED may additionally allow for a larger and more homogenous distribution of MNPs within the tumour. However, more work is necessary to ensure uniform distribution of the MNPs intratumourally, including a better understanding of their kinetics. Targeted MNPs may also permit more efficient targeting of tumour cells and improved MHT efficacy. Significant MHT modifications can be translated to further increased antitumour efficacy and the future use of this treatment modality in combination with other adjuvant therapies as part of the standard of care for GBM patients.

Conclusions

GBM has remained a formidable treatment challenge despite advances in surgery, RT and chemotherapy. MHT was first explored as a cancer treatment in the 1950s and has already been approved in Europe within the past 5 years as a treatment modality for patients with recurrent GBM. The MNPs used for MHT applications allow for a tumour-specific and prolonged therapeutic effect. Additionally, MHT can sensitise tumour cells to adjuvant therapies including RT and chemotherapy. These findings hold great promise and allow for further consideration of MHT as an adjuvant therapy for GBM in the United States.

References

1. Louis DN, Perry A, Reifenberger G, et al. The 2016 World Health Organization Classification of Tumors of the Central Nervous System: a summary. Acta Neuropathol. 2016; 131:803–20. [PubMed: 27157931]
2. Iacob G, Dinca EB. Current data and strategy in glioblastoma multiforme. J Med Life. 2009; 2:386–93. [PubMed: 20108752]
3. Ostrom QT, Gittleman H, Fulop J, et al. CBTRUS statistical report: primary brain and central nervous system tumors diagnosed in the United States in 2008–2012. Neuro-Oncology. 2015; 17(Suppl 4):iv1–62. [PubMed: 26511214]
4. Glioblastoma Multiforme. 2017. Available from: http://www.aans.org/Patients/Neurosurgical-Conditions-and-Treatments/Glioblastoma-Multiforme
5. Stupp R, Mason WP, van den Bent MJ, et al. Radiotherapy plus concomitant and adjuvant temozolomide for glioblastoma. N Engl J Med. 2005; 352:987–96. [PubMed: 15758009]
6. Jackson M, Hassiotou F, Nowak A. Glioblastoma stem-like cells: at the root of tumor recurrence and a therapeutic target. Carcinogenesis. 2015; 36:177–85. [PubMed: 25504149]
7. Hochberg FH, Pruitt A. Assumptions in the radiotherapy of glioblastoma. Neurology. 1980; 30:907–11. [PubMed: 6252514]
8. De Bacco F, D'Ambrosio A, Casanova E, et al. MET inhibition overcomes radiation resistance of glioblastoma stem-like cells. EMBO Mol Med. 2016; 8:550–68. [PubMed: 27138567]
9. Safari M, Khoshnevisan A. Cancer stem cells and chemoresistance in glioblastoma multiform: a review article. J Stem Cells. 2015; 10:271–85. [PubMed: 27144829]
10. Bao S, Wu Q, McLendon RE, et al. Glioma stem cells promote radioresistance by preferential activation of the DNA damage response. Nature. 2006; 444:756–60. [PubMed: 17051156]

11. Wang D, Berglund A, Kenchappa RS, et al. BIRC3 is a novel driver of therapeutic resistance in glioblastoma. Sci Rep. 2016; 6:21710. [PubMed: 26888114]
12. Kleihues P, Sobin LH. World Health Organization classification of tumors. Cancer. 2000; 88:2887. [PubMed: 10870076]
13. Stupp R, Hegi ME, Mason WP, et al. Effects of radiotherapy with concomitant and adjuvant temozolomide versus radiotherapy alone on survival in glioblastoma in a randomised phase III study: 5-year analysis of the EORTC-NCIC trial. Lancet Oncol. 2009; 10:459–66. [PubMed: 19269895]
14. Hadjipanayis CG, Widhalm G, Stummer W. What is the surgical benefit of utilizing 5-aminolevulinic acid for fluorescence-guided surgery of malignant gliomas? Neurosurgery. 2015; 77:663–73. [PubMed: 26308630]
15. Aminolevulinic acid hydrochloride, known as ALA HCl (Gleolan, NX Development Corp.) as an optical imaging agent indicated in patients with gliomas. 2017. Available from: https://www.fda.gov/Drugs/InformationOnDrugs/ApprovedDrugs/ucm562645.htm
16. Toraya-Brown S, Fiering S. Local tumour hyperthermia as immunotherapy for metastatic cancer. Int J Hyperthermia. 2014; 30:531–9. [PubMed: 25430985]
17. Roussakow S. The history of hyperthermia rise and decline. Conf Pap Med. 2013; 2013:1.
18. Attaluri A, Kandala SK, Wabler M, et al. Magnetic nanoparticle hyperthermia enhances radiation therapy: a study in mouse models of human prostate cancer. Int J Hyperthermia. 2015; 31:359–74. [PubMed: 25811736]
19. Gunderson L, Tepper J. Clinical radiation oncology. 3.
20. Skitzki JJ, Repasky EA, Evans SS. Hyperthermia as an immunotherapy strategy for cancer. Curr Opin Investig Drugs (Lond, England: 2000). 2009; 10:550–8.
21. Silva AC, Oliveira TR, Mamani JB, et al. Application of hyperthermia induced by superparamagnetic iron oxide nanoparticles in glioma treatment. Int J Nanomed. 2011; 6:591–603.
22. van der Zee J. Heating the patient: a promising approach? Ann Oncol. 2002; 13:1173–84. [PubMed: 12181239]
23. Kalamida D, Karagounis IV, Mitrakas A, et al. Fever-range hyperthermia vs. hypothermia effect on cancer cell viability, proliferation and HSP90 expression. PLoS ONE. 2015; 10:e0116021. [PubMed: 25635828]
24. Lee Titsworth W, Murad GJ, Hoh BL, et al. Fighting fire with fire: the revival of thermotherapy for gliomas. Anticancer Res. 2014; 34:565–74. [PubMed: 24510985]
25. Kampinga HH. Cell biological effects of hyperthermia alone or combined with radiation or drugs: a short introduction to newcomers in the field. Int J Hyperthermia. 2006; 22:191–6. [PubMed: 16754338]
26. Pu P-yZhang Y-zJiang D-h. Apoptosis induced by hyperthermia in human glioblastoma cell line and murine glioblastoma. Chin J Cancer Res. 2000; 12:257–62.
27. Fukami T, Nakasu S, Baba K, et al. Hyperthermia induces translocation of apoptosis-inducing factor (AIF) and apoptosis in human glioma cell lines. J Neurooncol. 2004; 70:319–31. [PubMed: 15662973]
28. Wang H-Y, Fu JC-M, Lee Y-C, et al. Hyperthermia stress activates heat shock protein expression via propyl isomerase 1 regulation with heat shock factor 1. Mol Cell Biol. 2013; 33:4889–99. [PubMed: 24126052]
29. Quanz M, Herbette A, Sayarath M, et al. Heat shock protein 90α (Hsp90α) is phosphorylated in response to DNA damage and accumulates in repair foci. J Biol Chem. 2012; 287:8803–15. [PubMed: 22270370]
30. Schmid TE, Multhoff G. Radiation-induced stress proteins – the role of heat shock proteins (HSP) in anti-tumor responses. CMC. 2012; 19:1765–70.
31. Hermisson M, Strik H, Rieger J, et al. Expression and functional activity of heat shock proteins in human glioblastoma multiforme. Neurology. 2000; 54:1357–65. [PubMed: 10746610]
32. Ampie L, Choy W, Lamano JB, et al. Heatshock protein vaccines against glioblastoma: from bench to bedside. J Neurooncol. 2015; 123:441–8. [PubMed: 26093618]

33. Bloch O, Lim M, Sughrue ME, et al. Autologous heat shock protein peptide vaccination for newly diagnosed glioblastoma: impact of peripheral PD-L1 expression on response to therapy. Clin Cancer Res. 2017; 23:3575. [PubMed: 28193626]
34. Iwata K, Shakil A, Hur WJ, et al. Tumour pO2 can be increased markedly by mild hyperthermia. Br J Cancer Suppl. 1996; 27:S217–S21. [PubMed: 8763884]
35. Krawczyk PM, Eppink B, Essers J, et al. Mild hyperthermia inhibits homologous recombination, induces BRCA2 degradation, and sensitizes cancer cells to poly (ADP-ribose) polymerase-1 inhibition. Proc Natl Acad Sci USA. 2011; 108:9851–6. [PubMed: 21555554]
36. Hermisson M, Wagenknecht B, Wolburg H, et al. Hyperthermia enhanced chemosensitivity of human malignant glioma cells. Anticancer Res. 2000; 19:2338–23.
37. Raaphorst GP, Chabot P, Doja S, et al. Effect of hyperthermia on cisplatin sensitivity in human glioma and ovarian carcinoma cell lines resistant and sensitive to cisplatin treatment. Int J Hyperthermia. 1996; 12:211–22. [PubMed: 8926390]
38. Man J, Shoemake JD, Ma T, et al. Hyperthermia sensitizes glioma stem-like cells to radiation by inhibiting AKT signaling. Cancer Res. 2015; 75:1760–9. [PubMed: 25712125]
39. Kampinga HH, Dikomey E. Hyperthermic radiosensitization: mode of action and clinical relevance. Int J Radiat Biol. 2001; 77:399–408. [PubMed: 11304434]
40. Mehta M, Khan A, Danish S, et al. Radiosensitization of primary human glioblastoma stem-like cells with low-dose AKT inhibition. Mol Cancer Ther. 2015; 14:1171–80. [PubMed: 25695954]
41. Raaphorst GP, Feeley MM. Hyperthermia radiosensitization in human glioma cells comparison of recovery of polymerase activity, survival, and potentially lethal damage repair. Int J Radiat Oncol Biol Phys. 1994; 29:133–9. [PubMed: 8175420]
42. Kaur P, Hurwitz MD, Krishnan S, et al. Combined hyperthermia and radiotherapy for the treatment of cancer. Cancers. 2011; 3:3799–823. [PubMed: 24213112]
43. Chatterjee DK, Diagaradjane P, Krishnan S. Nanoparticle-mediated hyperthermia in cancer therapy. Ther Deliv. 2011; 2:1001–14. [PubMed: 22506095]
44. Kozissnik B, Bohorquez AC, Dobson J, et al. Magnetic fluid hyperthermia: advances, challenges, and opportunity. Int J Hyperthermia. 2013; 29:706–14. [PubMed: 24106927]
45. Gilchrist RK, Medal R, Shorey WD, et al. Selective inductive heating of lymph nodes. Ann Surg. 1957; 146:596–606. [PubMed: 13470751]
46. Mahmoudi K, Hadjipanayis CG. The application of magnetic nanoparticles for the treatment of brain tumors. Front Chem. 2014; 2:109. [PubMed: 25520952]
47. Dennis CL, Ivkov R. Physics of heat generation using magnetic nanoparticles for hyperthermia. Int J Hyperthermia. 2013; 29:715–29. [PubMed: 24131317]
48. Carrey J, Mehdaoui B, Respaud M. Simple models for dynamic hysteresis loop calculations of magnetic single-domain nanoparticles: application to magnetic hyperthermia optimization. J Appl Phys. 2011; 109:083921.
49. Dormann JL, Fiorani D, Tronc E. Advances in chemical physics. Hoboken (NJ): John Wiley & Sons, Inc; 2007. Magnetic relaxation in fine-particle systems; 283–494.
50. Dennis CL, Krycka KL, Borchers JA, et al. Internal magnetic structure of nanoparticles dominates time-dependent relaxation processes in a magnetic field. Adv Funct Mater. 2015; 25:4300–11.
51. Hu R, Ma S, Li HU, et al. Effect of magnetic fluid hyperthermia on lung cancer nodules in a murine model. Oncol Lett. 2011; 2:1161–4. [PubMed: 22848282]
52. Kossatz S, Grandke J, Couleaud P, et al. Efficient treatment of breast cancer xenografts with multifunctionalized iron oxide nanoparticles combining magnetic hyperthermia and anti-cancer drug delivery. Breast Cancer Res. 2015; 17:66. [PubMed: 25968050]
53. Zadnik PL, Molina CA, Sarabia-Estrada R, et al. Characterization of intratumor magnetic nanoparticle distribution and heating in a rat model of metastatic spine disease. J Neurosurg Spine. 2014; 20:740–50. [PubMed: 24702509]
54. Jordan A, Scholz R, Maier-Hauff K, et al. The effect of thermotherapy using magnetic nanoparticles on rat malignant glioma. J Neurooncol. 2006; 78:7–14. [PubMed: 16314937]
55. Zhao Q, Wang L, Cheng R, et al. Magnetic nanoparticle-based hyperthermia for head & neck cancer in mouse models. Theranostics. 2012; 2:113–21. [PubMed: 22287991]

56. Wang L, Dong J, Ouyang W, et al. Anticancer effect and feasibility study of hyperthermia treatment of pancreatic cancer using magnetic nanoparticles. Oncol Rep. 2012; 27:719–26. [PubMed: 22134718]
57. Moroz P, Jones SK, Gray BN. Tumor response to arterial embolization hyperthermia and direct injection hyperthermia in a rabbit liver tumor model. J Surg Oncol. 2002; 80:149–56. [PubMed: 12115798]
58. Maier-Hauff K, Ulrich F, Nestler D, et al. Efficacy and safety of intratumoral thermotherapy using magnetic iron-oxide nanoparticles combined with external beam radiotherapy on patients with recurrent glioblastoma multiforme. J Neurooncol. 2011; 103:317–24. [PubMed: 20845061]
59. Jones EL, Oleson JR, Prosnitz LR, et al. Randomized trial of hyperthermia and radiation for superficial tumors. JCO. 2005; 23:3079–85.
60. Wang J. Simulation of magnetic nanoparticle hyperthermia in prostate tumors. 2014. Available from: https://jscholarship.library.jhu.edu/bitstream/handle/1774.2/37090/WANG-THESIS-2014.pdf?sequence=1&isAllowed=y
61. Giordano MA, Gutierrez G, Rinaldi C. Fundamental solutions to the bioheat equation and their application to magnetic fluid hyperthermia. Int J Hyperthermia. 2010; 26:475–84. [PubMed: 20578812]
62. Pennes HH. Analysis of tissue and arterial blood temperatures in the resting human forearm. J Appl Physiol (Bethesda, MD: 1985). 1948; 1:34–93.
63. Bellizzi G, Bucci OM. On the optimal choice of the exposure conditions and the nanoparticle features in magnetic nanoparticle hyperthermia. Int J Hyperthermia. 2010; 26:389–403. [PubMed: 20210609]
64. Maier-Hauff K, Rothe R, Scholz R, et al. Intracranial thermotherapy using magnetic nanoparticles combined with external beam radiotherapy: results of a feasibility study on patients with glioblastoma multiforme. J Neurooncol. 2007; 81:53–60. [PubMed: 16773216]
65. Stigliano RV, Shubitidze F, Petryk AA, et al. Magnetic nanoparticle hyperthermia: predictive model for temperature distribution. Proc Spie Int Soc Opt Eng. 2013; 8584:858410. [PubMed: 25301993]
66. Krishnan S, Diagaradjane P, Cho SH. Nanoparticle-mediated thermal therapy: evolving strategies for prostate cancer therapy. Int J Hyperthermia. 2010; 26:775–89. [PubMed: 20858069]
67. Serlin Y, Shelef I, Knyazer B, et al. Anatomy and physiology of the blood–brain barrier. Semin Cell Dev Biol. 2015; 38:2–6. [PubMed: 25681530]
68. Obermeier B, Daneman R, Ransohoff RM. Development, maintenance and disruption of the blood–brain barrier. Nat Med. 2013; 19:1584–96. [PubMed: 24309662]
69. van Tellingen O, Yetkin-Arik B, de Gooijer MC, et al. Overcoming the blood–brain tumor barrier for effective glioblastoma treatment. Drug Resist Updates. 2015; 19:1–12.
70. Qin DX, Zheng R, Tang J, et al. Influence of radiation on the blood–brain barrier and optimum time of chemotherapy. Int J Radiat Oncol Biol Phys. 1990; 19:1507–10. [PubMed: 2262373]
71. van Vulpen M, Kal HB, Taphoorn MJ, et al. Changes in blood–brain barrier permeability induced by radiotherapy: implications for timing of chemotherapy? Oncol Rep. 2002; 9:683–8. [PubMed: 12066192]
72. Bobo RH, Laske DW, Akbasak A, et al. Convection-enhanced delivery of macromolecules in the brain. Proc Natl Acad Sci USA. 1994; 91:2076–80. [PubMed: 8134351]
73. Vogelbaum MA, Aghi MK. Convection-enhanced delivery for the treatment of glioblastoma. Neuro-Oncology. 2015; 17:ii3–8. [PubMed: 25746090]
74. Debinski W, Tatter SB. Convection-enhanced delivery for the treatment of brain tumors. Expert Rev Neurother. 2009; 9:1519–27. [PubMed: 19831841]
75. Motion JPM, Huynh GH, Szoka FC, et al. Convection and retroconvection enhanced delivery: some theoretical considerations related to drug targeting. Pharm Res. 2011; 28:472–9. [PubMed: 20963628]
76. Lonser RR, Walbridge S, Garmestani K, et al. Successful and safe perfusion of the primate brainstem: in vivo magnetic resonance imaging of macromolecular distribution during infusion. J Neurosurg. 2002; 97:905–13. [PubMed: 12405380]

77. Saito R, Sonoda Y, Kumabe T, et al. Regression of recurrent glioblastoma infiltrating the brainstem after convection-enhanced delivery of nimustine hydrochloride. J Neurosurg Pediatr. 2011; 7:522–6. [PubMed: 21529193]

78. Sandberg DI, Edgar MA, Souweidane MM. Convection-enhanced delivery into the rat brainstem. J Neurosurg. 2002; 96:885–91. [PubMed: 12005396]

79. Jahangiri A, Chin AT, Flanigan PM, et al. Convection-enhanced delivery in glioblastoma: a review of preclinical and clinical studies. J Neurosurgneurosurg. 2017; 126:191–200.

80. Saito R, Krauze MT, Bringas JR, et al. Gadolinium-loaded liposomes allow for real-time magnetic resonance imaging of convection-enhanced delivery in the primate brain. Exp Neurol. 2005; 196:381–9. [PubMed: 16197944]

81. Bañobre-López M, Teijeiro A, Rivas J. Magnetic nanoparticle-based hyperthermia for cancer treatment. Rep Pract Oncol Radiother. 2013; 18:397–400. [PubMed: 24416585]

82. Pradhan P, Giri J, Banerjee R, et al. Cellular interactions of lauric acid and dextran-coated magnetite nanoparticles. J Magnet Magnet Mater. 2007; 311:282–7.

83. Wu W, Xiao XH, Zhang SF, et al. Synthesis and magnetic properties of maghemite (γ-Fe(2)O(3)) short-nanotubes. Nanoscale Res Lett. 2010; 5:1474–9. [PubMed: 20730115]

84. Kaluzova M, Bouras A, Machaidze R, et al. Targeted therapy of glioblastoma stem-like cells and tumor non-stem cells using cetuximab-conjugated iron-oxide nanoparticles. Oncotarget. 2015; 6:8788–806. [PubMed: 25871395]

85. Platt S, Nduom E, Kent M, et al. Canine model of convection-enhanced delivery of cetuximab conjugated iron-oxide nanoparticles monitored with magnetic resonance imaging. Clin Neurosurg. 2012; 59:107–13. [PubMed: 22960522]

86. Hadjipanayis CG, Machaidze R, Kaluzova M, et al. EGFRvIII antibody-conjugated iron oxide nanoparticles for magnetic resonance imaging-guided convection-enhanced delivery and targeted therapy of glioblastoma. Cancer Res. 2010; 70:6303–12. [PubMed: 20647323]

87. Bouras A, Kaluzova M, Hadjipanayis CG. Radiosensitivity enhancement of radioresistant glioblastoma by epidermal growth factor receptor antibody-conjugated iron-oxide nanoparticles. J Neurooncol. 2015; 124:13–22. [PubMed: 25981803]

88. Markides H, Rotherham M, El Haj AJ. Biocompatibility and toxicity of magnetic nanoparticles in regenerative medicine. J Nanomater. 2012; 2012:1.

89. Mahmoudi M, Laurent S, Shokrgozar MA, et al. Toxicity evaluations of superparamagnetic iron oxide nanoparticles: cell “vision” versus physicochemical properties of nanoparticles. ACS Nano. 2011; 5:7263–76. [PubMed: 21838310]

90. Laurent S, Burtea C, Thirifays C, et al. Crucial ignored parameters on nanotoxicology: the importance of toxicity assay modifications and “cell vision”. PLoS One. 2012; 7:e29997. [PubMed: 22253854]

91. Arbab AS, Yocum GT, Rad AM, et al. Labeling of cells with ferumoxides-protamine sulfate complexes does not inhibit function or differentiation capacity of hematopoietic or mesenchymal stem cells. NMR Biomed. 2005; 18:553–9. [PubMed: 16229060]

92. Castaneda RT, Boddington S, Henning TD, et al. Labeling human embryonic stem-cell-derived cardiomyocytes for tracking with MR imaging. Pediatr Radiol. 2011; 41:1384–92. [PubMed: 21594541]

93. Muldoon LL, Sandor M, Pinkston KE, et al. Imaging, distribution, and toxicity of superparamagnetic iron oxide magnetic resonance nanoparticles in the rat brain and intracerebral tumor. Neurosurgery. 2005; 57:785–96. discussion 785–96. [PubMed: 16239893]

94. Wang Q, Shen M, Zhao T, et al. Low toxicity and long circulation time of polyampholyte-coated magnetic nanoparticles for blood pool contrast agents. Sci Rep. 2015; 5:7774. [PubMed: 25585607]

95. Bernd H, De Kerviler E, Gaillard S, et al. Safety and tolerability of ultrasmall superparamagnetic iron oxide contrast agent: comprehensive analysis of a clinical development program. Invest Radiol. 2009; 44:336–42. [PubMed: 19661843]

96. Shinkai M, Yanase M, Honda H, et al. Intracellular hyperthermia for cancer using magnetite cationic liposomes: in vitro study. Japan J Cancer Res: GANN. 1996; 87:1179–83. [PubMed: 9045948]

97. Ito A, Shinkai M, Honda H, et al. Heat shock protein 70 expression induces antitumor immunity during intracellular hyperthermia using magnetite nanoparticles. Cancer Immunol Immunother: CII. 2003; 52:80–8. [PubMed: 12594571]

98. Meenach SA, Hilt JZ, Anderson KW. Poly(ethylene glycol)-based magnetic hydrogel nanocomposites for hyperthermia cancer therapy. Acta Biomater. 2010; 6:1039–46. [PubMed: 19840875]

99. Xu H, Zong H, Ma C, et al. Evaluation of nanomagnetic fluid on malignant glioma cells. Oncol Lett. 2017; 13:677–80. [PubMed: 28356945]

100. Yanase M, Shinkai M, Honda H, et al. Intracellular hyperthermia for cancer using magnetite cationic liposomes: ex vivo study. Japan J Cancer Res: GANN. 1997; 88:630–2. [PubMed: 9310134]

101. Yanase M, Shinkai M, Honda H, et al. Intracellular hyperthermia for cancer using magnetite cationic liposomes: an in vivo study. Japan J Cancer Res: GANN. 1998; 89:463–9. [PubMed: 9617354]

102. Yanase M, Shinkai M, Honda H, et al. Antitumor immunity induction by intracellular hyperthermia using magnetite cationic liposomes. Japan J Cancer Res: GANN. 1998; 89:775–82. [PubMed: 9738985]

103. Le B, Shinkai M, Kitade T, et al. Preparation of tumor-specific magnetoliposomes and their application for hyperthermia. J Chem Eng Japan/JCEJ. 2001; 34:66–72.

104. Ohno T, Wakabayashi T, Takemura A, et al. Effective solitary hyperthermia treatment of malignant glioma using stick type CMC-magnetite. In vivo study. J Neurooncol. 2002; 56:233–9. [PubMed: 12061729]

105. Rabias I, Tsitrouli D, Karakosta E, et al. Rapid magnetic heating treatment by highly charged maghemite nanoparticles on Wistar rats exocranial glioma tumors at microliter volume. Biomicrofluidics. 2010; 4:024111. [PubMed: 20697578]

106. Ohtake M, Umemura M, Sato I, et al. Hyperthermia and chemotherapy using Fe(Salen) nanoparticles might impact glioblastoma treatment. Sci Rep. 2017; 7:42783. [PubMed: 28218292]

107. Jiang H, Wang C, Guo Z, et al. Silver nanocrystals mediated combination therapy of radiation with magnetic hyperthermia on glioma cells. J Nanosci Nanotechnol. 2012; 12:8276–81. [PubMed: 23421206]

108. Sato I, Umemura M, Mitsudo K, et al. Simultaneous hyperthermia-chemotherapy with controlled drug delivery using single-drug nanoparticles. Sci Rep. 2016; 6:24629. [PubMed: 27103308]

109. Ito A, Shinkai M, Honda H, et al. Heat-inducible TNF-alpha gene therapy combined with hyperthermia using magnetic nanoparticles as a novel tumor-targeted therapy. Cancer Gene Ther. 2001; 8:649–54. [PubMed: 11593333]

110. Luethy JD, Fargnoli J, Park JS, et al. Isolation and characterization of the hamster gadd153 gene. Activation of promoter activity by agents that damage DNA. J Biol Chem. 1990; 265:16521–6. [PubMed: 2398062]

111. Nemkov V, Ruffini R, Goldstein R, et al. Magnetic field generating inductor for cancer hyperthermia research. Int J Comput Math Electr Electron Eng. 2011; 30:1626–36.

112. Bonvin D, Alexander DTL, Millán A, et al. Tuning properties of iron oxide nanoparticles in aqueous synthesis without ligands to improve MRI relaxivity and SAR. Nanomaterials. 2017; 7:225.

113. Thiesen B, Jordan A. Clinical applications of magnetic nanoparticles for hyperthermia. Int J Hyperthermia. 2008; 24:467–74. [PubMed: 18608593]

114. Bordelon DE, Goldstein RC, Nemkov VS, et al. Modified solenoid coil that efficiently produces high amplitude AC magnetic fields with enhanced uniformity for biomedical applications. IEEE Trans Magn. 2012; 48:47–52. [PubMed: 25392562]

115. Gneveckow U, Jordan A, Scholz R, et al. Description and characterization of the novel hyperthermia- and thermoablation-system MFH 300F for clinical magnetic fluid hyperthermia. Med Phys. 2004; 31:1444–51. [PubMed: 15259647]

116. Wust P, Gneveckow U, Johannsen M, et al. Magnetic nanoparticles for interstitial thermotherapy – feasibility, tolerance and achieved temperatures. Int J Hyperthermia. 2006; 22:673–85. [PubMed: 17390997]

117. Johannsen M, Gneveckow U, Eckelt L, et al. Clinical hyperthermia of prostate cancer using magnetic nanoparticles: presentation of a new interstitial technique. Int J Hyperthermia. 2005; 21:637–47. [PubMed: 16304715]

118. Johannsen M, Gneveckow U, Thiesen B, et al. Thermotherapy of prostate cancer using magnetic nanoparticles: feasibility, imaging, and three-dimensional temperature distribution. Eur Urol. 2007; 52:1653–61. [PubMed: 17125906]

119. Fighting cancer more effectively and with fewer side effects. Available from: http://www.magforce.de/en/produkte/nanotherm-therapie.html

120. Trefná HD, Crezee H, Schmidt M, et al. Quality assurance guidelines for superficial hyperthermia clinical trials: I. Clinical requirements. Int J Hyperthermia. 2017; 33:471–82.

121. Dobšíček Trefná H, Crezee J, Schmidt M, et al. Quality assurance guidelines for superficial hyperthermia clinical trials: II. Technical requirements for heating devices. Strahlenther Onkol. 2017; 193:351–66. [PubMed: 28251250]

122. Obaidat MI, Issa B, Haik Y. Magnetic properties of magnetic nanoparticles for efficient hyperthermia. Nanomaterials. 2015; 5:63–89. [PubMed: 28347000]

123. Atkinson WJ, Brezovich IA, Chakraborty DP. Usable frequencies in hyperthermia with thermal seeds. IEEE Trans Biomed Eng. 1984; BME-31:70–5.

124. Hergt R, Dutz S. Magnetic particle hyperthermia—biophysical limitations of a visionary tumour therapy. J Magnet Magnet Mater. 2007; 311:187–92.

125. Ortega D, Pankhurst QA. Nanoscience: volume 1: nanostructures through chemistry. Vol. 1. Cambridge (UK): The Royal Society of Chemistry; 2013. Magnetic hyperthermia; 60–88.

126. van Landeghem FK, Maier-Hauff K, Jordan A, et al. Postmortem studies in glioblastoma patients treated with thermo-therapy using magnetic nanoparticles. Biomaterials. 2009; 30:52–7. [PubMed: 18848723]

127. Grauer O, Jaber M, Hess K, et al. RTHP-22. Inflammatory response after modified nanotherm and radiotherapy of recurrent glioblastoma. Neuro-Oncology. 2016; 18:vi178–9.

128. Beinart R, Nazarian S. Effects of external electrical and magnetic fields on pacemakers and defibrillators: from engineering principles to clinical practice. Circulation. 2013; 128:2799–809. [PubMed: 24366589]

129. Liu H, Zhang J, Chen X, et al. Application of iron oxide nanoparticles in glioma imaging and therapy: from bench to bedside. Nanoscale. 2016; 8:7808–26. [PubMed: 27029509]

130. Lagendijk JJW, Mooibroek J, Crezee J. Future developments in respect of thermal modeling, treatment planning, and treatment control for interstitial hyperthermia. In: Seegenschmiedt MH, Sauer R, editorsInterstitial and intracavitary thermoradiotherapy. Berlin, Heidelberg: Springer Berlin Heidelberg; 1993. 155–9.

131. Hunt JW, Lalonde R, Ginsberg H, et al. Rapid heating: critical theoretical assessment of thermal gradients found in hyperthermia treatments. Int J Hyperthermia. 1991; 7:703–18. [PubMed: 1940506]

132. Attaluri A, Ivkov R, Ma R. , et al. Nanoparticle redistribution during magnetic nanoparticle hyperthermia: multi-physics porous medium model analyses. ASME International Mechanical Engineering Congress and Exposition, Volume 7: Fluids and Heat Transfer, Parts A, B, C, and D;

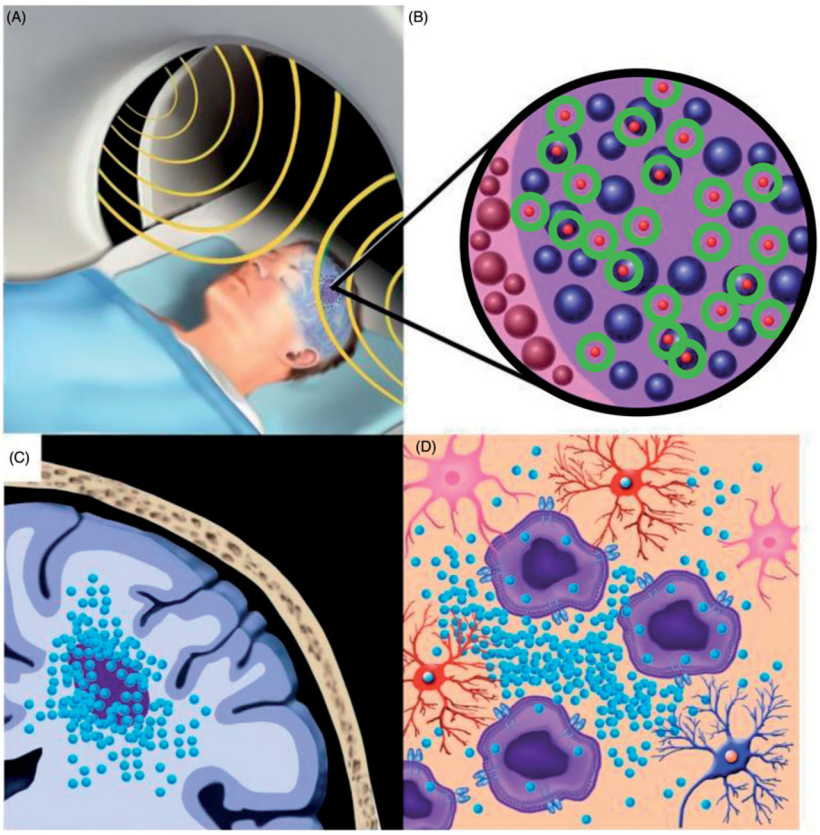

Figure 1.

MHT in a patient with a malignant brain tumour. (A) Following the delivery of MNPs to the tumour site, the patient's head is positioned within an AMF generator. (B) Heat is produced (circles) by MNPs (small spheres) mainly through magnetic hysteresis losses. (C) The localised delivery of MNPs (small spheres) via convection-enhanced delivery (CED) results in a high concentration of MNPs in and around the tumour site. (D) The uptake of MNPs (small spheres) by tumour cells (large structures with a dark center) and macrophages (not shown) results in an enhanced cellular response to heat. Adapted from [46].

Table 1

Data comparison of *in vitro* studies performed to evaluate the application of MHT for the treatment of gliomas.

Study	Tumour Cell Line	Magnetic nanoparticle composition	Iron concentration (mg/ml)	Temperature reached (°C)	Magnetic field frequency (kHz)	Magnetic field intensity (kA/m)	Duration of AMF exposure (min)	Results
Shinkai *et al.* [96]	T-9	Magnetite cationic liposomes	7.2, 7.5, 10	42.6, 43.9, 44.8	118	30.6	40–60	No viable tumour cells remained
Ito *et al.* [97]	T-9	Magnetite cationic liposomes	0.1	42.0	118	30.6	30	Tumour cell apoptosis and necrosis
Meenach *et al.* [98]	M059K	Polyethylene glycol-based magnetic hydrogel nanocomposites	1.58, 1.92, 2.74, 5.32, 7.24, 7.93	60.7, 59.5, 65.7, 66.1, 73.8, 79.6	297	18–25	5	Tumour cell thermo-ablation
Xu *et al.* [99]	U251	Iron oxide	2, 4, 6, 8	40, 42, 44, 46	200	Not specified	60	Tumour cell apoptosis and necrosis

Table 2

Data comparison of animal studies performed to evaluate the application of MHT for the treatment of gliomas.

Study	Tumour cell line	Animal model	Tumour cells implantation site	Magnetic nanoparticle composition	Iron concentration (mg/ml)	Temperature reached (°C)	Magnetic field frequency (kHz)	Magnetic field intensity (kA/m)	Duration of AMF exposure (min)	Results
Yanase *et al.* [100]	T-9	F344 rats	Subcutaneously in the left femoral region	Magnetite cationic liposomes	0.2	43	118	30.6	60	Complete glioma cell death
Yanase *et al.* [101]	T-9	F344 rats	Subcutaneously in the left femoral region	Magnetite cationic liposomes	0.4	43–44	118	30.6	30	Necrotic tumour cells; some animals displayed complete tumour regression
Yanase *et al.* [102]	T-9	F344 rats	Subcutaneously in the left and right femoral region	Magnetite cationic liposomes	7.5	43–44	118	30.6	30	Some animals displayed complete tumour regression
Shinkai *et al.* [96]	T-9	F344 rats	Subcutaneously in the left and right femoral region	Magnetite cationic liposomes	7.5	43–44	118	30.6	30	Some animals displayed complete tumour regression
Ito *et al.* [97]	T-9	F344 rats	Subcutaneously in the left femoral region	Magnetite cationic liposomes	7.5	42	118	30.6	30	Reduced tumour growth in the immunised animal group
Le *et al.* [103]	U251-SP	Athymic nude mice	Subcutaneously in the femoral region	Magnetite cationic liposomes	5	43	118	30.6	30	Complete tumour growth suppression
Ohno *et al.* [104]	T-9	F344 rats	Orthotopic	Carboxymethyl-cellulose magnetite	5.8	44.4	88.9	30.6	30	Significant tumour cell death
Rabias *et al.* [105]	C6	Wistar rats	Subcutaneously in the area anterior to the bregma	Maghemite	20	Not specified	150	11	20	Tumour tissue damage and dissolution
Jordan *et al.* [54]	RG-2	F344 rats	Orthotopic	Aminosilane-coated nanoparticles	Not specified	45	100	18	40	Necrotic tumour tissue
Xu *et al.* [99]	U251	Rats	Subcutaneously in right lower limb	Iron oxide	2, 4, 6, 8	Not specified	200	Not specified	60	Reduced tumour growth

Table 3

Data comparison of clinical studies using MHT in patients with GBM.

Study	Number of patients	Magnetic nanoparticle composition	Median injected volume of magnetic fluid (ml)	Iron concentration (mg/ml)	Magnetic field frequency (kHz)	Magnetic field intensity (kA/m)	AMF duration (min) per session	Total number of AMF sessions	Median survival rate (months)
Maier-Hauff *et al.* [64]	14	Aminosilane coated superparamagnetic iron oxide nanoparticles dispersed in water	3	112	100	2.5–18	60	4–10	14.5
Maier-Hauff *et al.* [58]	59	Aminosilane coated superparamagnetic iron oxide nanoparticles dispersed in water	4.5	112	100	2.0–15	60	6	23.2
van Landeghem *et al.* [126]	3	Aminosilane coated superparamagnetic iron oxide nanoparticles dispersed in water	4.5	112	100	2.5–18	60	6	n/a